Electron binding energies and Dyson orbitals of $Al_5O_m^-$ $(m=3, 4, 5)$ and $Al_5O_5H_2^-$

Cite as: J. Chem. Phys. **127**, 234302 (2007); https://doi.org/10.1063/1.2806845
Submitted: 30 July 2007 . Accepted: 16 October 2007 . Published Online: 18 December 2007

Alfredo Guevara-García, Ana Martínez, and J. V. Ortiz

Electron binding energies and Dyson orbitals of $Al_5O_m^-$ (m=3,4,5) and $Al_5O_5H_2^-$

Alfredo Guevara-García and Ana Martínez
Instituto de Investigaciones en Materiales, Universidad Nacional Autónoma de México, Circuito Exterior Sin Número, Ciudad Umversitaria, P.O. Box 70-360 Coyoacán, 04510 Distrito Federal, Mexico

J. V. Ortiz[a)]
Department of Chemistry and Biochemistry, Auburn University, Auburn, Alabama 36849-5312, USA

(Received 30 July 2007; accepted 16 October 2007; published online 18 December 2007)

Photoelectron spectra of $Al_5O_m^-$ (m=3–5) and of the anion produced by the dissociative adsorption of a water molecule by $Al_5O_4^-$ are interpreted with density-functional geometry optimizations and electron-propagator calculations of vertical electron detachment energies. For $Al_5O_3^-$, $Al_5O_4^-$, and $Al_5O_5H_2^-$, the observed signals may be attributed to the most stable isomer of each anion. For $Al_5O_5^-$, the features in the photoelectron spectrum are due to three almost isoenergetic isomers. © *2007 American Institute of Physics*. [DOI: 10.1063/1.2806845]

INTRODUCTION

Aluminum and oxygen are among the most abundant elements on the surface of the Earth. Aluminum artifacts have been ubiquitous in modern civilization for more than a century. Catalyst supports and reactive surfaces often have a component of aluminum oxide. Interfaces between aluminum and alumina (Al_2O_3) occur whenever the bulk metal is exposed to oxygen. Spectroscopic and theoretical studies of aluminum-oxygen clusters are especially relevant to understanding these interfaces when the Al:O atomic ratio exceeds $\frac{2}{3}$. Such metal-rich clusters may have formal Al oxidation states between +3 and 0.

Photoelectron spectra of metal-rich cluster anions[1,2] exhibit features that might have been expected to correlate with simple notions of electron counting. In this view, a closed-shell metal-rich $Al_nO_m^-$ cluster, where n is odd should have a number of peaks corresponding to low vertical electron detachment energies (VEDEs) that is equal to the number of electron pairs that are left to the Al atoms after assigning a charge of −2 to each O atom: $(3n+1-2m)/2$. Subsequent experimental studies[3–5] have confirmed this supposition to some extent, but theoretical investigation has established the complicating presence of more than one isomer in mass-selected samples.[6–12] Even before these findings were published, photoisomerization between two forms of $Al_3O_3^-$ had been demonstrated[2] through modulation of relative peak intensities with respect to variation of the conditions of anion preparation. Hole-burning experiments confirmed this interpretation.[3]

Recent photoelectron experiments have considered the reactivity of anionic clusters. Preparation of $Al_3O_3^-$ followed by reactions with water, methanol, and ammonia molecules yields anionic clusters whose masses correspond to addition products.[13,14] Photoelectron spectra of the latter species and theoretical studies[15–18] have shown that protic nucleophiles add dissociatively to $Al_3O_3^-$. More recent experiments and accompanying calculations[19] have considered spectra of $Al_5O_4^-$ and the product formed from the reaction of this anion with a water molecule.

In this work, we interpret experiments on the two latter anions and examine two experimentally characterized clusters[5] that also have five Al atoms, $Al_5O_3^-$ and $Al_5O_5^-$. In addition to optimizing stable minima for these anions, VEDEs are determined with electron propagator methods. The latter techniques also provide Dyson orbitals that correspond to each transition energy and that facilitate interpretation of correlated *ab initio* predictions in terms of rigorous one-electron concepts.

METHODS

Geometry optimizations on singlet anions without symmetry constraints were performed with the GAUSSIAN03 program[20] in the B3LYP/6-311+G($2d,p$) approximation.[21,22] Previous work indicates that such optimizations are likely to provide accurate results.[9–12] To locate transition states, the synchronous transit-guided quasi-Newton method[23] was used. Optimized minima and transition states were confirmed with harmonic frequency analysis. These geometries were assumed in electron propagator[24,25] calculations of the vertical electron detachment energies (VEDEs). Two self-energy approximations were employed: the outer valence Green's function[26,27] (OVGF) and partial third order (P3).[28,29] The 6-311+G($2df,p$) basis set was used in both cases. Pole strengths exceeded 0.85 in all cases and therefore confirmed the qualitative validity of the P3 and OVGF calculations. Structural diagrams and Dyson orbital plots were generated with BALL & STICK[30] and MOLDEN,[31] respectively.

OVGF results for VEDEs are generally larger than P3 values by 0.3 eV or less, but both methods lead to the same assignments. Closer agreement with experimental data may occur with one method or the other for a given cluster anion.

[a)]Electronic mail: ortiz@auburn.edu.

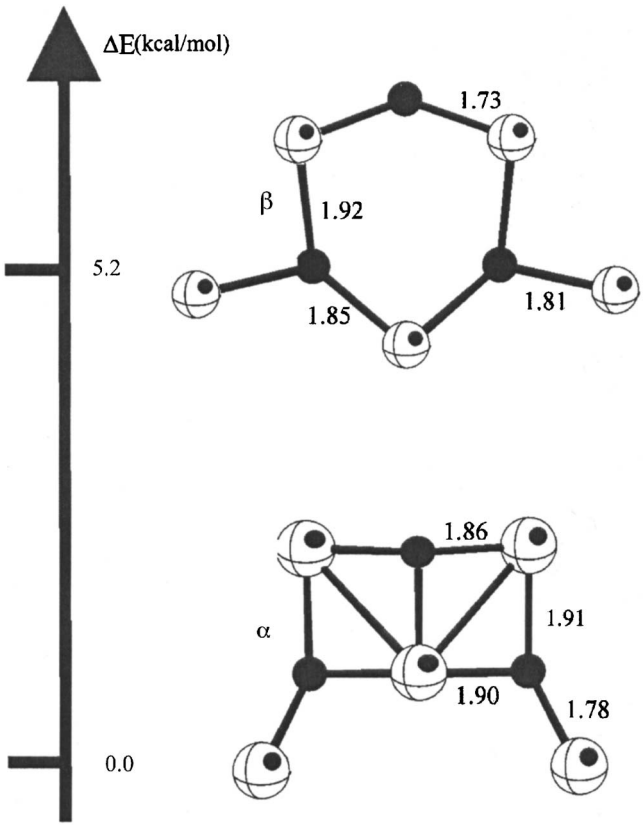

FIG. 1. B3LYP/6-311+G(2d) structures and relative energies (kcal/mol) of $Al_5O_3^-$. Bond distances are in Å.

In the absence of experimental data, the P3 and OVGF values might provide estimated lower and upper bounds to experimental VEDEs.

RESULTS AND DISCUSSION

$Al_5O_3^-$

Figure 1 shows the most stable structures for $Al_5O_3^-$. The lowest isomer (α) resembles the $Al_3O_3^-$ *book* structure reported previously[9] except for the two terminal Al atoms. The α isomer has C_s symmetry, while the β isomer has C_{2v} symmetry. The energy difference between these two isomers is 5.2 kcal/mol.

Table I summarizes the VEDE calculations. Experimental and Koopmans' theorem (KT) values also are shown. The corresponding Dyson orbitals are displayed in Figs. 2 and 3.

As can be seen in Table I, the VEDEs from isomer α match pretty well with the experimental values. In this case,

TABLE I. $Al_5O_3^-$ vertical electron detachment energies (eV).

Anion	Final state	KT	P3	OVGF	Expt.[a]
α	$^2A'$	2.63	2.41	2.57	2.56
	$^2A''$	3.55	3.33	3.62	3.39
	$^2A'$	4.14	3.89	4.18	4.31
β	$^2B_2$	3.06	2.84	3.09	
	$^2A_1$	3.36	3.09	3.34	
	$^2A_1$	3.80	3.58	3.85	

[a]Reference 5.

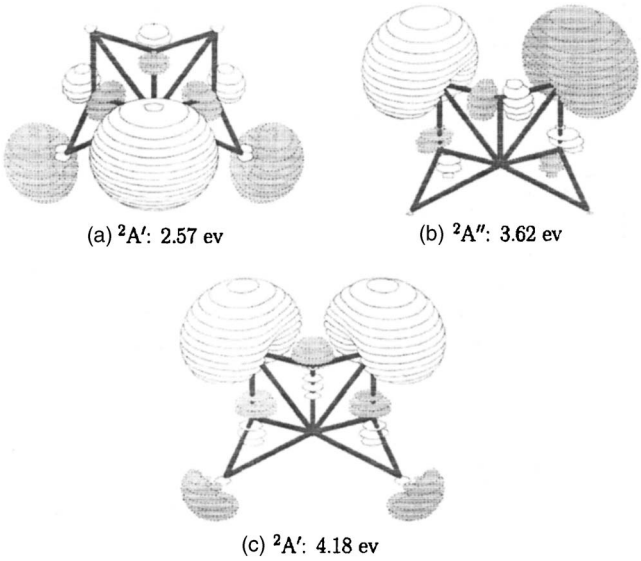

FIG. 2. Dyson orbitals for isomer α of $Al_5O_3^-$. The final states after electron detachment and the associated OVGF/6-311+G(2*df*) VEDEs are shown.

the OVGF approximation seems to be the best. The associated Dyson orbitals consist chiefly of Al 3*s* functions. Previous studies of related anions suggest that there are five Al-centered Dyson orbitals and that the two most strongly bound consist of bonding and antibonding combinations of 3*s* functions on the two least-coordinated metal centers. VEDEs for these Dyson orbitals are beyond the energy range of the experimental spectrum. Next in energy are the bonding and antibonding combinations of Al 3*s* functions on the corner sites, where each metal atom has two oxygen neighbors. Finally, for the lowest VEDE, the Dyson orbital is localized chiefly on the central Al, which has the highest oxygen coordination number. The latter Dyson orbital also displays opposite-phase contributions from terminal Al 3*s* functions.

For isomer β, the calculated VEDEs have larger devia-

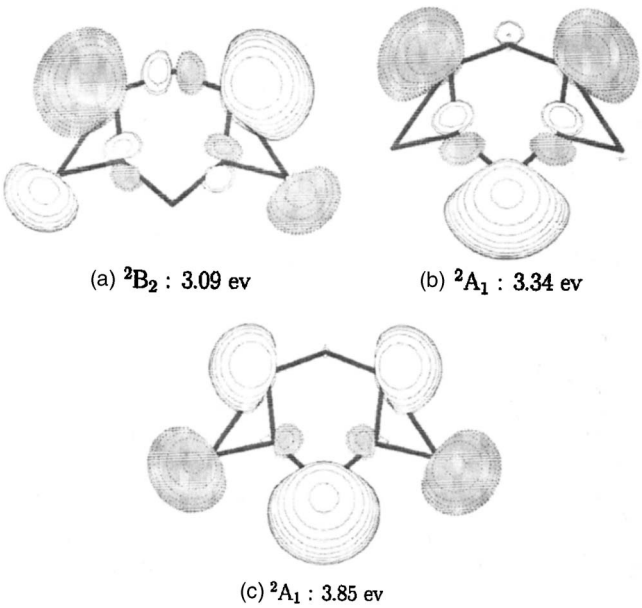

FIG. 3. Dyson orbitals for isomer β of $Al_5O_3^-$. The final states after electron detachment and the associated OVGF/6-311+G(2*df*) VEDEs are shown.

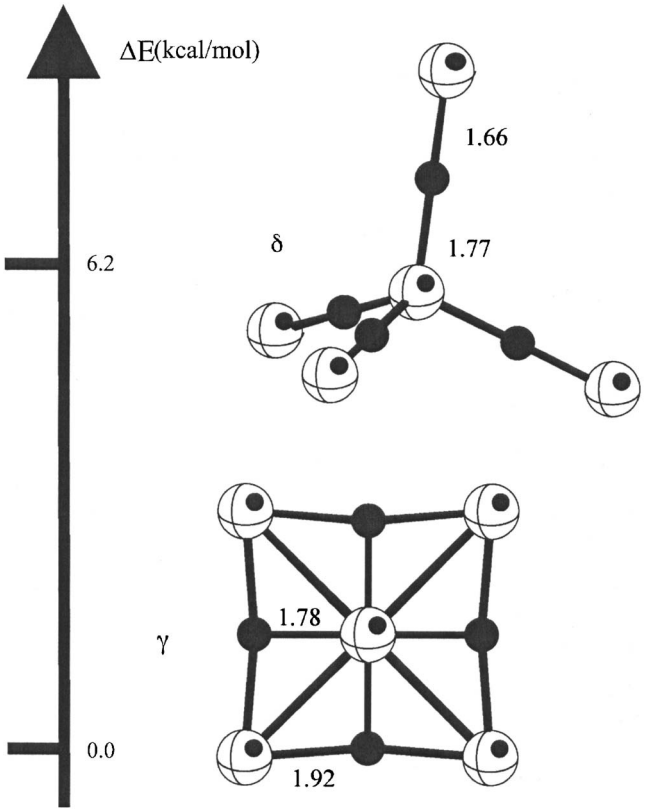

FIG. 4. B3LYP/6-311+G(2*d*) structures and relative energies (kcal/mol) of $Al_5O_4^-$. Bond distances are in Å.

tions from the experimental values. These results do not conclusively establish the irrelevancy of this isomer to the $Al_5O_3^-$ photoelectron spectra for they occur in a region where the spectra show a continuous signal. The isomerization energy of 5.2 kcal/mol is not sufficiently large to remove the β isomer from consideration. However, one may conclude that the α isomer is chiefly responsible for the features observed in the photoelectron spectrum of $Al_5O_3^-$. The five Al-centered Dyson orbitals in the β isomer display a similar ordering with respect to oxygen coordination number, but in this case there are two terminal metal centers with only one oxygen neighbor and three ring metal centers with two oxygen neighbors. The Dyson orbitals for the lowest three VEDEs correspond to combinations of Al 3*s* functions on the ring centers.

$Al_5O_4^-$

Optimized structures of $Al_5O_4^-$ are shown in Fig. 4. The most stable structure, γ, is almost planar, but slight displacements of the oxygens from the Al plane give it D_{2d} symmetry. Isomer δ has T_d symmetry. These results are similar to those obtained by Das *et al.*[19]

Table II shows calculated VEDEs for $Al_5O_4^-$ isomers along with experimental data. The corresponding Dyson orbitals are displayed in Figs. 5 and 6.

In Table II, the first two calculated VEDEs for isomer γ are in good agreement with the experimental values. The P3 approximation works best in this case. The two features observed in the spectrum of Meloni *et al.*[5] can be assigned to

TABLE II. $Al_5O_4^-$ vertical electron detachment energies (eV).

Anion	Final state	KT	P3	OVGF	Expt.[a]	Expt.[b]
γ	$^2B_1$	3.91	3.76	4.00	3.83	3.72 (X)
	^2E	4.09	3.91	4.14	3.99	4.94 (A)
	$^2A_1$	4.95	4.83	5.08		4.30 (B)
δ	$^2T_2$	4.99	4.97	5.25		
	$^2A_1$	5.20	5.21	5.49		

[a]Reference 5.
[b]Reference 19.

the two lowest VEDEs of this isomer. In the spectrum of Das *et al.*,[19] the two lowest VEDEs of isomer γ match well with the two lowest features. The B peak observed at 4.3 eV in the latter experiment[19] does not appear to have a counterpart in the other report[5] and may not necessarily correspond to a vertical transition. The P3 and OVGF predictions for the $^2A_1$ final state lie outside the energy range of these experiments. Dyson orbitals for the $^2B_1$, ^2E, and $^2A_1$ final states consist chiefly of Al 3*s* functions with minor antibonding oxygen contributions. Phase relationships in these orbitals are determined by symmetry.

For isomer δ, the calculated VEDEs are irrelevant to the spectra for they exceed the experimental photon energy, 4.66 eV. Therefore, isomer δ may be present, but not detected. However, isomer δ cannot account for the observed VEDEs. Symmetry criteria also determine the phase relationships between Al 3*s* functions in the Dyson orbitals that correspond to the $^2T_2$ and $^2A_1$ final states.

$Al_5O_5H_2^-$

Das *et al.*[19] reported photoelectron spectra for species generated by the reaction between $Al_5O_4^-$ and H_2O. They

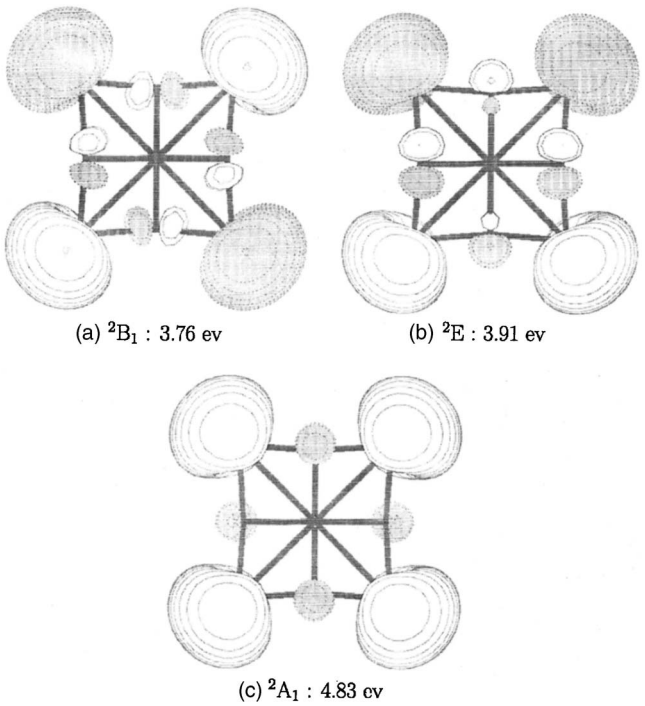

FIG. 5. Dyson orbitals for isomer γ of $Al_5O_4^-$. The final states after electron detachment and the associated P3/6-311+G(2*df*) VEDEs are shown.

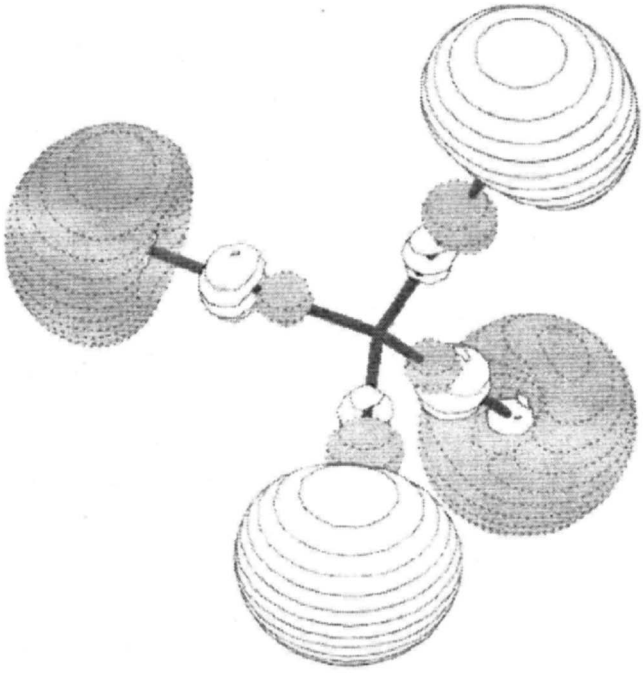

FIG. 6. Dyson orbitals for isomer δ of $Al_5O_4^-$. The final states after electron detachment and the associated P3/6-311+G(2*df*) VEDEs are shown.

found that water is dissociatively adsorbed on γ-$Al_5O_4^-$, leading to the most stable $Al_5O_5H_2^-$ isomer, which has a C_s symmetry (see Fig. 7). Their density-functional theory (DFT) and time-dependent density-functional theory (TDDFT) results are shown in Table III. VEDEs for $Al_5O_5H_2^-$ calculated with the P3 and OVGF electron propagator approximations, experimental data, and KT values also are shown. The corresponding Dyson orbitals are displayed in Fig. 8.

Nucleophilic attack on $Al_3O_3^-$ occurs at the metal atom with the lowest amplitudes in the two Al-centered Dyson

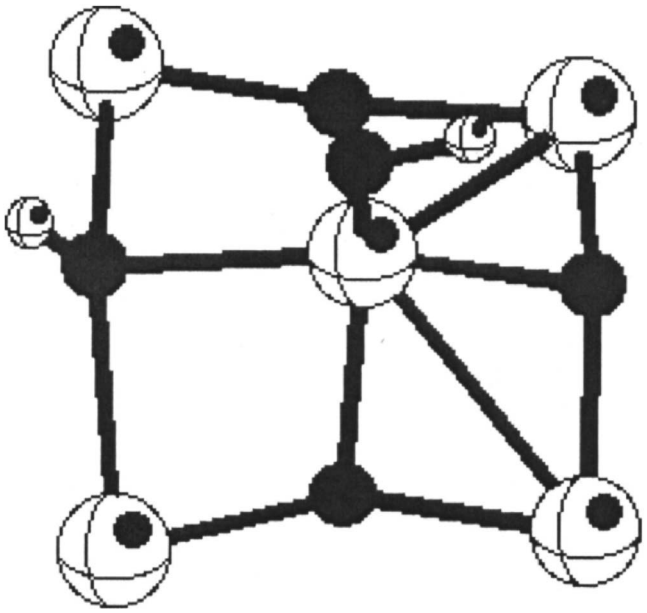

FIG. 7. B3LYP/6-311+G(2*d*,*p*) structure of $Al_5O_5H_2^-$.

orbitals.[13–18] A proton transfer to a neighboring oxygen atom follows for nucleophiles such as H_2O and NH_3. A similar outcome occurs here and results in a cluster with two hydroxide ligands, one bound to the central Al atom and another that is coordinated to three metal centers.

P3 results agree closely with the experimental values for the first three VEDEs. A fourth final state is predicted to lie outside the 4.66 eV limit imposed by the photon energy. An accurate separation between the second and third VEDEs is obtained. Dyson orbitals for the first two VEDEs consist chiefly of 3*s* functions on the two Al centers without an OH neighbor; the lowest VEDE corresponds to the antibonding combination. For the third and fourth VEDEs, the Dyson orbitals consist of 3*s* functions on the other two corner Al atoms.

$Al_5O_5^-$

Figure 9 shows the most stable $Al_5O_5^-$ structures. The most stable isomer, ϵ, has a C_{2v} symmetry. Isomers ζ, η, and θ have C_s, C_{2v}, and C_s symmetries, respectively.

The three lowest isomers have closely related structures (see Fig. 10). Reduction of one Al–O–Al angle in isomer ϵ to form a four-member ring leads to isomer ζ. Another such reduction connects the latter structure to isomer η. The activation barrier between isomers ζ and ϵ is 2.4 kcal/mol, and the one between isomers η and ζ is 1 kcal/mol. These values may be underestimated by the B3LYP procedure.

TABLE III. $Al_5O_5H_2^-$ vertical electron detachment energies (eV).

KT	P3	OVGF	DFT-TDDFT	Expt.[a]
3.56	3.38	3.64	3.13	3.37
4.02	3.82	4.08	3.36	3.72
4.53	4.35	4.57	3.52	4.20
5.16	5.01	5.24	4.31	

[a]Reference 19.

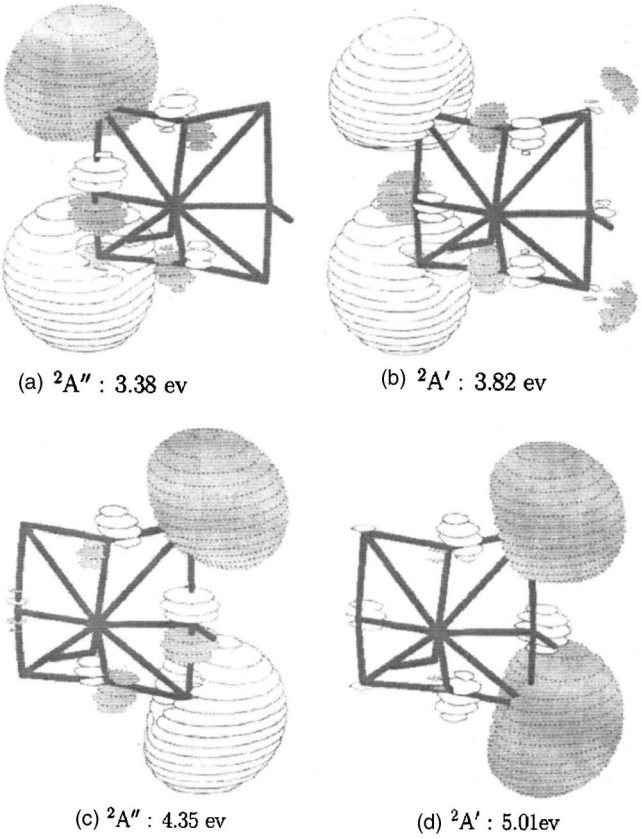

FIG. 8. Dyson orbitals for $Al_5O_5H_2^-$. The final states after electron detachment and the associated P3/6-311+G($2df,p$) VEDEs are shown.

Table IV displays VEDEs calculated with the P3, OVGF, and KT approximations and experimental results. The corresponding Dyson orbitals are displayed in Figs. 11–13.

Table IV shows that, for isomer ϵ, there is only one VEDE that is lower than the experimental photon energy (4.66 eV). The difference between the P3 and the OVGF values is 0.3 eV. The VEDE obtained with the OVGF approximation is closer to the experimental value of 2.22 eV. For isomer ζ, the calculated VEDEs using the OVGF approximation are in good agreement with the experimental values of 2.91 and 3.74 eV. The third VEDE of this isomer is out of the experimental detection range. In the case of isomer η, the three lowest VEDEs have energies that are lower than the experimental photon energy. The lowest VEDE may contribute to shoulders on the B or C peaks. The next two VEDEs may be assigned to the feature observed at 4.26 eV. A contribution to the spectrum by isomer θ's first VEDE cannot be discounted, for its total energy is close to that of isomer η.

In the ϵ, ζ, and η isomers, Dyson orbitals for the three lowest VEDEs consist chiefly of Al 3s functions. In this set of transitions, lower oxygen coordination numbers are associated with higher VEDEs. In the ϵ isomer, the large distance between the two terminal Al atoms produces a small difference between the second and third VEDEs. Lower symmetry in the ζ case yields Dyson orbitals that are localized on the terminal Al or on the Al centers with only two oxygen neighbors. With C_{2v} symmetry restored in isomer η, there is extensive delocalization among the three Al atoms with two oxygen neighbors. For all of these structures, nucleophilic attack is most likely at the two Al centers that are next to three oxygen atoms.

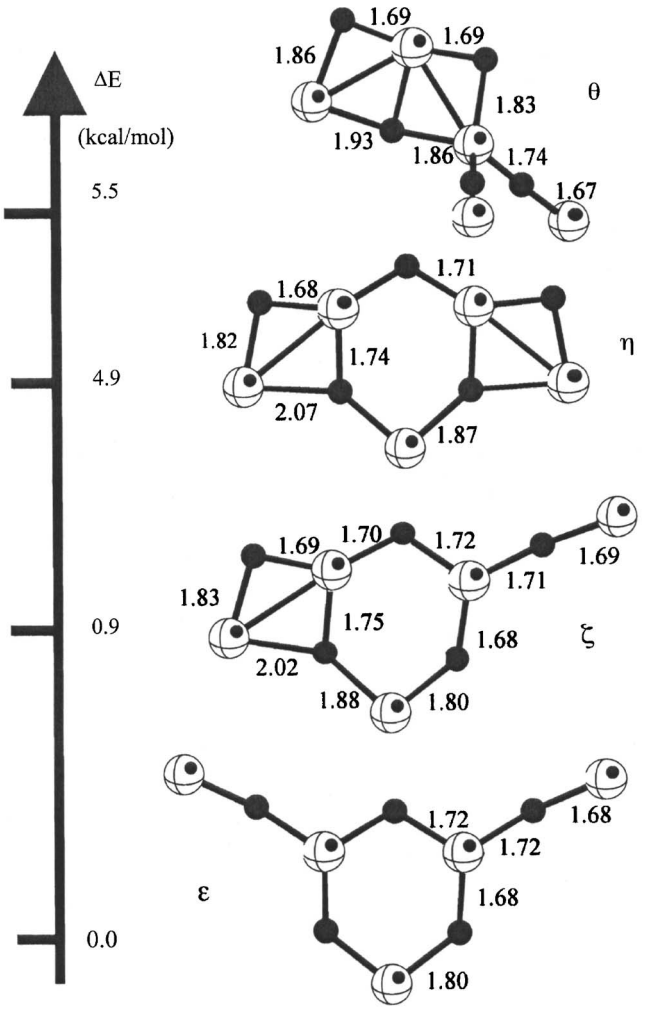

FIG. 9. B3LYP/6-311+G(2d) structures and relative energies (kcal/mol) of $Al_5O_5^-$. Bond distances are in Å.

CONCLUSIONS

Electron propagator calculations on the VEDEs of structure α suffice for an assignment of the photoelectron spectrum[5] of $Al_5O_3^-$. Whereas the β structure's total energy is only 5 kcal/mol higher, its VEDEs are not in agreement with the observed spectral features. For the lowest VEDE, the corresponding Dyson orbital is localized chiefly on the Al atom with the highest number of oxygen neighbors. Bonding and antibonding combinations of Al 3s functions on the sites with two oxygen neighbors are the chief constituents of the Dyson orbitals for the next two VEDEs. Electron counting

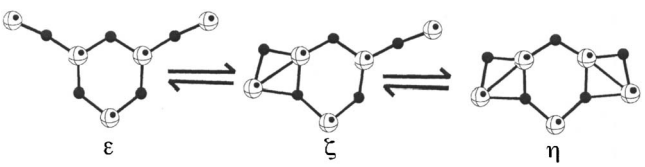

FIG. 10. Structural relationships between the three lowest isomers of $Al_5O_5^-$.

TABLE IV. $Al_5O_5^-$ vertical electron detachment energies (eV).

Anion	KT	P3	OVGF	Expt.[a]
ϵ	1.91	1.78	2.13	2.22 (A)
	6.08	6.11	6.32	
	6.10	6.14	6.35	
ζ	2.71	2.56	2.86	2.91 (B)
	3.64	3.52	3.79	3.74 (C)
	6.43	6.49	6.70	
η	3.35	3.18	3.44	
	4.06	3.93	4.18	4.26 (D)
	4.34	4.22	4.48	4.26 (D)
θ	3.42	3.34	3.63	
	5.47	5.47	5.71	
	5.57	5.59	5.83	

[a]Reference 5.

rules imply that there are five Al-localized Dyson orbitals and therefore two higher VEDEs that are inaccessible in recent experiments await further study. The Dyson orbitals for these two VEDEs are likely to be localized on the terminal Al atoms.

Peaks in the photoelectron spectra of $Al_5O_4^-$ (Refs. 5 and 19) may be assigned to VEDEs of the γ isomer. This D_{2d} structure is nearly planar. The first two transitions correspond to $^2B_1$ and ^2E final states. Predictions on the third VEDE are markedly higher (and out of the energetic range of the reported experiments) than a third feature seen in one spectrum.[19] Therefore, this feature may arise from geometrical relaxation or Jahn-Teller effects in the ^2E final states. Dyson orbitals consist chiefly of symmetry-adapted combinations of 3*s* functions on the corner Al atoms with small antibonding contributions from oxygen 2*s* or 2*p* functions. Isomer δ's VEDEs are too high to account for any of the observed transitions.

Because the contributions of the central Al to the γ isomer's Dyson orbitals are negligible, nucleophilic attack by a water molecule is most likely at this position. After a proton transfer to a neighboring oxygen atom, the resulting C_s minimum has two hydroxide ligands, one attached to the central Al atom and another that is coordinated to three metal centers. P3 electron propagator calculations of VEDEs for this structure provide an accurate account of the three principal features seen in the experiment.[19] Four Dyson orbitals are symmetry-adapted combinations of corner Al 3*s* functions.

Four peaks in the photoelectron spectrum[5] of $Al_5O_5^-$ reflect the presence of several isomers which are separated by low barriers. The lowest peak may be assigned to the first VEDE of the ϵ isomer. Whereas the ζ isomer is only 0.9 kcal/mole less stable, one may ascribe the second and third spectral peaks to the first two VEDEs of this structure. Accounting for the fourth observed peak is somewhat problematic, for the second and third VEDEs predicted for the η isomer are in reasonable agreement with its transition energy. This structure is only 4.9 kcal/mol higher than the ϵ isomer. However, the first VEDE of the η isomer therefore must be assigned to shoulder regions of the second or third peaks.

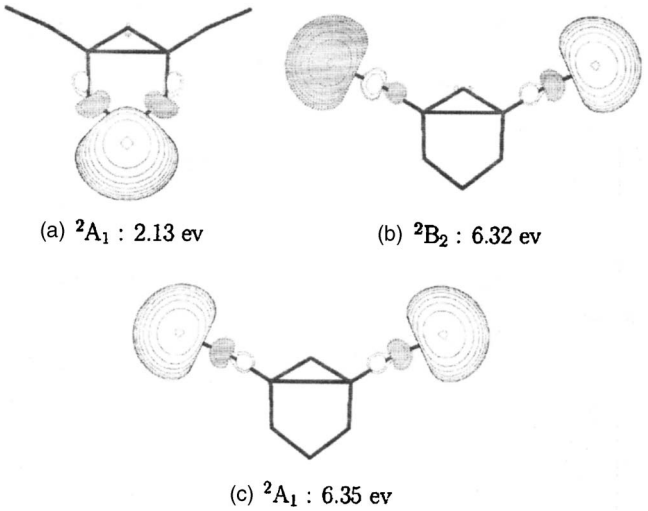

FIG. 11. Dyson orbitals for isomer ϵ of $Al_5O_5^-$. The final states after electron detachment and the associated OVGF/6-311+G(2*df*) VEDEs are shown.

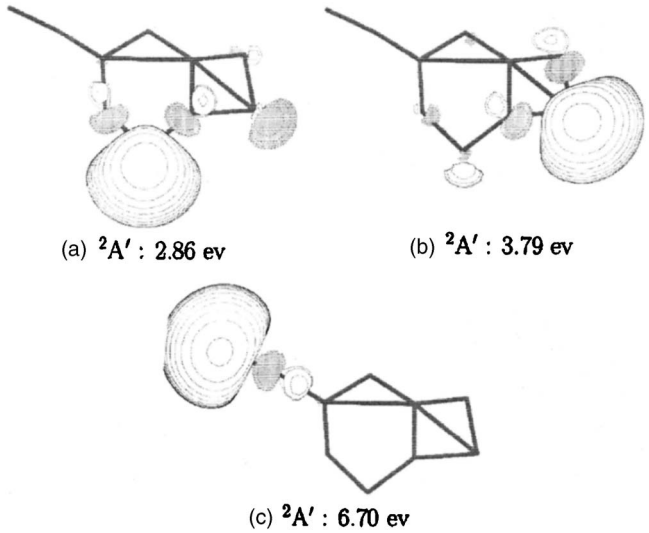

FIG. 12. Dyson orbitals for isomer ζ of $Al_5O_5^-$. The final states after electron detachment and the associated OVGF/6-311+G(2*df*) VEDEs are shown.

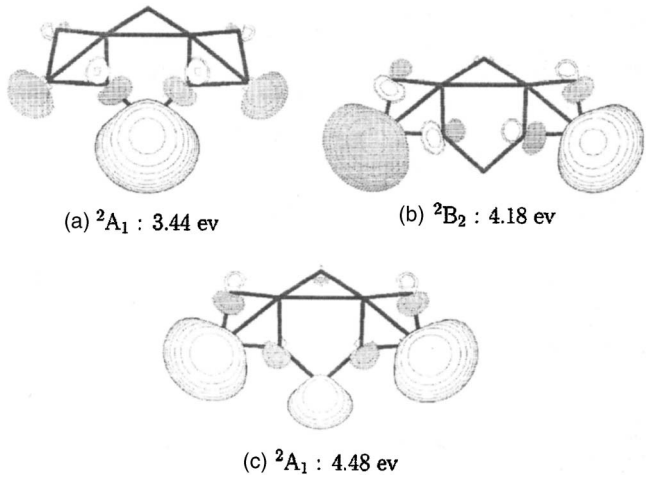

FIG. 13. Dyson orbitals for isomer η of $Al_5O_5^-$. The final states after electron detachment and the associated OVGF/6-311+G(2*df*) VEDEs are shown.

This explanation admits the possibility that the θ isomer also may make contributions to the spectrum. Each isomer has three VEDEs which correspond to Dyson orbitals that are localized on Al atoms. Higher VEDEs are associated with low oxygen coordination numbers.

ACKNOWLEDGMENTS

The authors would like to acknowledge Sara Jiménez Cortés and María Teresa Vázquez for technical support and DGSCA/UNAM (México) for providing computer time. This work was partially funded by DGAPA (No. IN107399) and CONACYT-NSF (E120.1778/2001). The National Science Foundation provided support through Grant No. CHE-0451810 to Auburn University. A.G.-G. would like to thank CONACYT for scholarship support.

[1] S. R. Desai, H. Wu, C. M. Rohlfing, and L. S. Wang, J. Chem. Phys. **106**, 1309 (1997).
[2] H. Wu, X. Li, X. B. Wang, C. F. Ding, and L. S. Wang, J. Chem. Phys. **109**, 449 (1998).
[3] F. A. Akin and C. C. Jarrold, J. Chem. Phys. **118**, 1773 (2003).
[4] F. A. Akin and C. C. Jarrold, J. Chem. Phys. **118**, 5841 (2003).
[5] G. Meloni, M. J. Ferguson, and D. M. Neumark, Phys. Chem. Chem. Phys. **5**, 4073 (2003).
[6] T. K. Ghanty and E. R. Davidson, J. Phys. Chem. A **103**, 2867 (1999).
[7] T. K. Ghanty and E. R. Davidson, J. Phys. Chem. A **103**, 8985 (1999).
[8] X. Y. Cui, I. Morrison, and J. G. Han, J. Chem. Phys. **117**, 1077 (2002).
[9] A. Martínez, F. J. Tenorio, and J. V. Ortiz, J. Phys. Chem. A **105**, 8787 (2001).
[10] A. Martínez, F. J. Tenorio, and J. V. Ortiz, J. Phys. Chem. A **105**, 11291 (2001).
[11] A. Martínez, L. E. Sansores, R. Salcedo, F. J. Tenorio, and J. V. Ortiz, J. Phys. Chem. A **106**, 10630 (2002).
[12] A. Martínez, F. J. Tenorio, and J. V. Ortiz, J. Phys. Chem. A **107**, 2589 (2003).
[13] F. A. Akin and C. C. Jarrold, J. Chem. Phys. **120**, 8698 (2004).
[14] R. B. Wyrwas, C. C. Jarrold, U. Das, and K. Ragavachari, J. Chem. Phys. **124**, 201101 (2006).
[15] F. J. Tenorio, I. Murray, A. Martínez, K. J. Klabunde, and J. V. Ortiz, J. Chem. Phys. **120**, 7955 (2004).
[16] A. Guevara-García, A. Martínez, and J. V. Ortiz, J. Chem. Phys. **122**, 214309 (2005).
[17] A. Guevara-García, A. Martínez, and J. V. Ortiz, J. Chem. Phys. **124**, 214304 (2006).
[18] A. Guevara-García, A. Martínez, and J. V. Ortiz, J. Chem. Phys. **126**, 024309 (2007).
[19] U. Das, K. Ragavachari, and C. C. Jarrold, J. Chem. Phys. **122**, 014313 (2005).
[20] M. J. Frisch, G. W. Trucks, H. B. Schlegel *et al.*, GAUSSIAN03, Revision B.05, Gaussian, Inc., Pittsburgh, PA, 2003.
[21] A. D. Becke, J. Chem. Phys. **98**, 5648 (1993); C. Lee, W. Yang, and R. G. Parr, Phys. Rev. B **37**, 785 (1988); B. Mielich, A. Savin, H. Stoll, and H. Preuss, Chem. Phys. Lett. **157**, 200 (1989).
[22] R. Krishnan, J. S. Binkley, R. Seeger, and J. A. Pople, J. Chem. Phys. **72**, 650 (1980); T. Clark, J. Chandrasekhar, G. W. Spitznagel, and P. V. R. Schleyer, J. Comput. Chem. **4**, 294 (1983); M. J. Frisch, J. A. Pople, and J. S. Binkley, J. Chem. Phys. **80**, 3265 (1984); A. D. McLean and G. S. Chandler, *ibid.* **72**, 5639 (1980).
[23] C. Peng, P. Y. Ayala, H. B. Schlegel, and M. J. Frisch, J. Comput. Chem. **17**, 49 (1996); C. Peng and H. B. Schlegel, Isr. J. Chem. **33**, 449 (1993).
[24] J. Linderberg and Y. Öhrn, *Propagators in Quantum Chemistry*, 2nd ed. (Wiley, Hoboken, NJ, 2004).
[25] J. V. Ortiz, Adv. Quantum Chem. **35**, 33 (1999).
[26] W. von Niessen, J. Schirmer, and L. S. Cederbaum, Comput. Phys. Rep. **1**, 57 (1984).
[27] J. V. Ortiz, in *Computational Chemistry: Reviews of Current Trends*, edited by J. Leszczynski (World Scientific, Singapore, 1997), Vol. 2, pp. 1–61.
[28] J. V. Ortiz, J. Chem. Phys. **104**, 7599 (1996).
[29] A. M. Ferreira, G. Seabra, O. Dolgounitcheva, V. G. Zakrzewski, and J. V. Ortiz, in *Quantum-Mechanical Prediction of Thermochemical Data*, edited by J. Cioslowski (Kluwer, Dordrecht, 2001), p. 131.
[30] N. Müller and A. Falk, BALL & STICK 3.7.6, molecular graphics software for MACOS, Johannes Kepler University, Linz, Austria, 2000.
[31] G. Schaftenaar and J. H. Noordik, J. Comput.-Aided Mol. Des. **14**, 123 (2000).